



Application of a New Trigonometric Theory in the Buckling Analysis of Three-Dimensional Thick Plate

Onyeka, F.C.¹, Okafor, F.O.² and Onah H.N.³

¹Department of Civil Engineering, Edo State University Uzairue, Edo State, Nigeria.

²Department of Civil Engineering, University of Nigeria Nsukka, Nigeria.

³Department of Civil Engineering, University of Nigeria Nsukka, Nigeria.

(Corresponding author: Onyeka, F.C.)

(Received 08 December 2020, Revised 26 January 2021, Accepted 27 February 2021)

(Published by Research Trend, Website: www.researchtrend.net)

ABSTRACT: In this paper, a new trigonometric shear deformation plate theory is developed for the buckling analysis of a three dimensional thick rectangular isotropic plate, elastically restrained along one edge and other three edges simply supported (CSSS) under uniaxial compressive load, using the variational Energy approach. Total potential energy equation of a thick plate was formulated from the three-dimensional constitutive relations, thereafter the compatibility equations was established to obtain the relations between the out of plane displacement and shear deformation slope along the direction of x and y coordinates. This total potential energy functional was differentiated with respect to deflection to obtain the governing equation. The functions for these slopes were obtained from out of plane function using the solution of compatibility equations while the solution of the governing equation is the function for the out of plane displacement. Finally, the total potential energy is minimized with respect to displacement coefficients, thereafter, the deflection and rotations were substituted back into the buckling equation derived to obtain the formulas for calculating the critical buckling load and other the mentioned functions. The three dimensional analysis for critical buckling of thick plates were carried out by varying parameters stiffness properties and aspect ratios. The proposed method obviates the need of shear correction factors which is associated with first order shear deformation theory for the energy equation formulation. The present theory unlike refined plate theories, considered all the stress elements of the plate in the analysis. From the numerical analysis obtained, it is found that the value of the critical buckling load increase as the span- thickness ratio increases. This suggests that as the thickness increases, the safety of the plate structure is improved.

Keywords: CSSS plate, a new trigonometric plate theory, compatibility and governing equation, three-dimensional buckling analysis, potential energy functional.

I. INTRODUCTION

The use of thick plate materials in engineering is on the increase over the years due to its attractive properties such as light weight, economy, its ability to withstand heavy loads and ability to tailor the structural properties, etc. Plate structures can be used in roof and floor slabs, bridge deck slabs, foundation footings, bulkheads, water tanks, ship hulls and spacecraft panels.

Plates can be classified into thick, membranes and thin plates, depending upon the heaviness of the plate [1].

In-plane loading causes a plate to buckle or become elastically unstable. The plates are mostly subjected to transverse and compressive loads acting in the middle plane of the plate. When a plate is subjected to forces applied at the boundary parallel to the mid-plane of the plate and distributed uniformly over the plate's thickness, the state of loading is called an in-plane compressive loading [2]. If the in-plane compressive load applied to the plate are further increased beyond their critical values, very large deflections and bending stresses will occur which will eventually lead to complete failure of the plate. To avoid failure of the

plate, relatively more accurate and practical studies on stability analysis of plate are required.

The classical plate theory (CPT) based on Kirchhoff assumptions [3-4] are normally used to plates analysis. It was discovered the solutions based on the classical theory agree well with the full elasticity solutions (away from the edges of the plate), provided the plate thickness is small relative to its other linear dimensions. The (CPT) neglect the effect of shear deformation which makes it inconsistent in the sense that elements are assumed to remain perpendicular to the mid-plane, yet the equilibrium requires that stress component which would cause these elements to deform still arise. In other words, the thin plate model still makes the assumption that normal stress and strain along the z axis (σ_z, ϵ_z) are zero. It was also assumed that the transverse shear stress (τ_{yz}) are zero. This assumption has discovered to have introduced errors, hence does not offer a very accurate analysis of plates in which the thickness-to length proportion is relatively large [5-6]. When the plate is relatively thick, one is advised to use an exact theory, for example one of the shear deformation theories.

In this theory, there is the added complication that vertical line elements before deformation do not have to remain perpendicular to the mid-surface after deformation, although they do remain straight [7; 8; 9]. Thus shear strains are generated, constant through the thickness of the plate. Also, Mindlin's theory satisfies constitutive relations for transverse shear stresses and shear strains by using shear correction factor.

In avoiding shear correction factor and to get the realistic variation of the transverse shear strains and stresses through the thickness of the plate for improved reliability in the thick plate analysis, higher order shear deformation plate theory (HSDT) evolved [10; 11; 12; 13; 14;15]. In their solution for the bending and buckling analysis of shear deformable plates, it was discovered that the thick plate model assumption does not offer a more reliable analysis of plates in which the thickness-to-length proportion is very heavy, therefore called incomplete three-dimensional analysis.

However, a thick plate is a typical three dimensional element and true analysis demands a complete three-dimensional analogy. A typical 3-D plate theory considered a deformation of the plate in the three directions (x, y, and z) thereby involves the twelve (12) stress/strain components in the analysis. That is, using complete three dimensional element for the analysis. It can be recorded that both first order theory (Mindlin's theory) and other higher shear deformation incomplete three-dimensional analysis are approximations of the exact three-dimensional equations of elasticity, but for a typical thick plate analysis, a typical 3-D plate theory is required [16].

Equally well, no much work has been performed along a typical three dimensional element stability analysis of thick plate by determining the exact displacement function from the compatibility equation to find out the outcome of critical buckling load.

Furthermore, the trigonometric displacement functions can be applied successfully to solve any boundary condition of rectangular plate; a feat that could not be easily achieved using exponential and hyperbolic shape functions. In addition, it is really necessary to adopt variational method to simplify a complex equations in the thick plate analysis because the integration of double Fourier series is quite involving unlike the present approach.

The author in [16] studied the 3-D elasticity buckling solution for simply supported thick rectangular plates using displacement potential functions approach and an assumed displacement functions, thereafter the governing differential equations were established using separation of variables method and satisfying the exact boundary conditions, an analytical solution is obtained

for linear elastic buckling of simply supported rectangular thick plates. They neither derive the displacement function from the compatibility equation, nor solve for isotropic plates elastically restrained along one the edge and other three edges simply supported. This gap in the literature is worth filling.

This work is aimed at bridging the gap in literature by developing a new trigonometric displacement theory and applied in the exact three-dimensional stability analysis of isotropic thick rectangular plate subjected to an in-plane loading. The main objective of this study is to determine a realistic formula for calculating the critical buckling load of thick rectangular plate elastically restrained along one the edge and other three edges simply supported (CSSS) under uniaxial compressive load, using the variational Energy approach. The study sought to achieve the main through the following specific objectives:

- To generate the potential energy of a three dimensional rectangular thick plate.
- To formulate the general governing and compatibility equations of the plate and obtain equations for the coefficients of deflection and shear deformation slope for x and y coordinates.
- To determine the expressions for the critical buckling load of the plate.

II. MATERIAL AND METHODS

A. Methodology

The processes involved in the formulation of the total potential energy of a thick rectangular plate includes kinematics relations and three-dimensional constitutive relations; formulation of strain energy and Potential energy.

Basic assumptions. The basic assumptions for three dimensional analyses of refined shear deformation thick continuum plate of small deflection theorems include the following:

- (i) The plate material is elastic, homogenous and isotropic.
- (ii) The middle surface of the flat plate never stretches nor compresses before, during or after bending.
- (iii) A flat x-z or y-z section, which is normal to middle x-y plane before bending shall no longer remain normal to the middle x-y surface after bending.

Kinematics Relations. Our formulation of energy equation for the stability analysis thick rectangular plate under compressive load will be based on figure 1, figure 2 and assumptions made in the previous section. As shown in figure 1, the spatial dimensions of the plate along x, y and z-axes are a, b and t respectively.

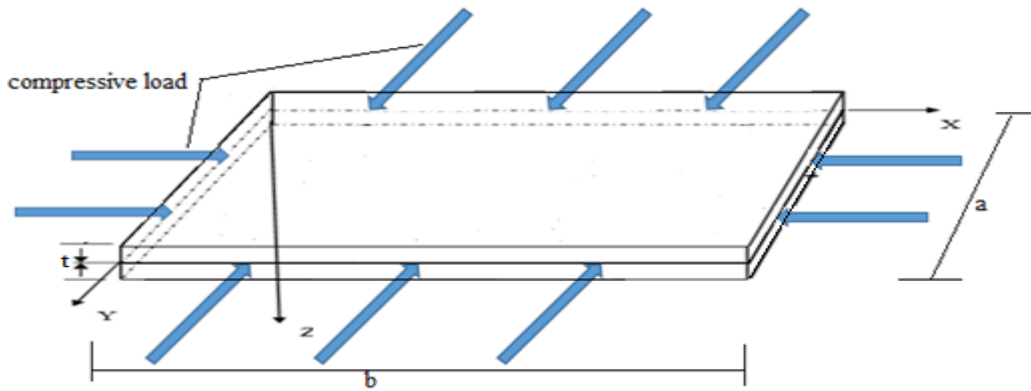


Fig. 1. A rectangular thick plate element showing the in-plane compressive loading.

As shown in the figure 2, the displacement field includes the displacements along x, y and z-axes: u, v and w respectively. The displacement and slope along the x axis and y axis are mathematically expressed as:

$$w = w(x, y, z) = hA_1 \quad (1)$$

$$\theta_x = \frac{\partial u}{\partial z} \quad (2)$$

$$\theta_y = \frac{\partial v}{\partial z} \quad (3)$$

Considering assumption iii and figure 1, F as used is a function of z coordinate. Thus, the in-plane displacements; u and v as presented in the Equation 2 and 3 are further defined using trigonometric relations for small angles as:

$$u = F(z)\theta_x = z\theta_x \quad (4)$$

$$v = F(z)\theta_y = z\theta_y \quad (5)$$

Where:

The symbol w denotes deflection, the symbol u denotes in-plane displacement along x-axis, the symbol v denotes in-plane displacement along y-axis, the symbol θ_x denotes shear deformation rotation along x axis, the symbol θ_y denotes shear deformation rotation along the y axis, and F denotes shear deformation profile.

Substituting Equation 2 and 3 into Equation 4 and 5 gives:

$$u = F(z) \frac{\partial u}{\partial z} \quad (6)$$

$$v = F(z) \frac{\partial v}{\partial z} \quad (7)$$

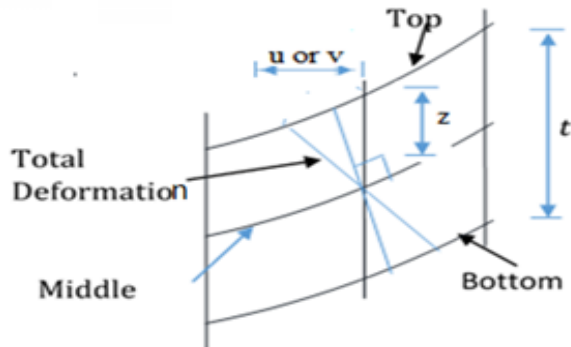


Fig. 2. Displacement of x-z (or y-z).

Taking the non-dimensional form of coordinates to be $R = x/a$, $Q = y/b$ and $S = z/t$ corresponding to x, y and z-axes respectively, the six strain components in terms of non-dimensional coordinates are written as:

$$\varepsilon_x = \frac{St}{a} \frac{d\theta_x}{dR} \quad (8)$$

$$\varepsilon_y = \frac{St}{a\beta} \frac{d\theta_y}{dQ} \quad (9)$$

$$\varepsilon_z = \frac{1}{t} \frac{dw}{dS} \quad (10)$$

$$\gamma_{xy} = \frac{St}{a\beta} \frac{d\theta_x}{dQ} + \frac{St}{a} \frac{d\theta_y}{dR} \quad (11)$$

$$\gamma_{xz} = \theta_x + \frac{1}{a} \frac{dw}{dR} \quad (12)$$

$$\gamma_{yz} = \theta_y + \frac{1}{a\beta} \frac{dw}{dQ} \quad (13)$$

Where:

the symbol ε_x denotes normal strain along x axis, the symbol ε_y denotes normal strain along y axis, the symbol ε_z denotes normal strain along z axis, the symbol γ_{xy} denotes shear strain in the plane parallel to the x-y plane, the symbol γ_{xz} denotes shear strain in the plane parallel to the x-z plane, the symbol γ_{yz} denotes shear strain in the plane parallel to the y-z plane.

Constitutive Relations. In the constitutive relation, the stresses causing the body movements are considered here. These stresses are described using generalized Hooke's law, therefore, the three dimensional constitutive relation for isotropic material is given as:

$$\begin{bmatrix} \sigma_x \\ \sigma_y \\ \sigma_z \\ \tau_{xz} \\ \tau_{yz} \\ \tau_{xy} \end{bmatrix} = \frac{1}{E} \begin{bmatrix} 1 & -\mu & -\mu & 0 & 0 & 0 \\ -\mu & 1 & -\mu & 0 & 0 & 0 \\ -\mu & -\mu & 1 & 0 & 0 & 0 \\ 0 & 0 & 0 & 2(1+\mu) & 0 & 0 \\ 0 & 0 & 0 & 0 & 2(1+\mu) & 0 \\ 0 & 0 & 0 & 0 & 0 & 2(1+\mu) \end{bmatrix} \begin{bmatrix} \varepsilon_x \\ \varepsilon_y \\ \varepsilon_z \\ \gamma_{xz} \\ \gamma_{yz} \\ \gamma_{xy} \end{bmatrix} \quad (14)$$

Young's modulus of elasticity and Poisson's ratios are denoted with E and μ respectively.

Substituting Equations 8 to 13 into Equation 14 and writing the equations of the six stress components one by one in term of the displacements gives:

$$\sigma_x = \frac{Ets}{(1+\mu)(1-2\mu)a} \left[(1-\mu) \cdot \frac{\partial \theta_x}{\partial R} + \frac{\mu}{\beta} \cdot \frac{\partial \theta_y}{\partial Q} + \frac{\mu a}{st^2} \cdot \frac{\partial w}{\partial S} \right] \quad (15)$$

$$\sigma_y = \frac{Ets}{(1+\mu)(1-2\mu)a} \left[\mu \cdot \frac{\partial \theta_x}{\partial R} + \frac{(1-\mu)}{\beta} \cdot \frac{\partial \theta_y}{\partial Q} + \frac{\mu a}{st^2} \cdot \frac{\partial w}{\partial S} \right] \quad (16)$$

$$\sigma_z = \frac{Ets}{(1+\mu)(1-2\mu)a} \left[\mu \cdot \frac{\partial \theta_x}{\partial R} + \frac{\mu}{\beta} \cdot \frac{\partial \theta_y}{\partial Q} + \frac{(1-\mu)a}{st^2} \cdot \frac{\partial w}{\partial S} \right] \quad (17)$$

$$\tau_{xy} = \frac{E(1-2\mu)ts}{2(1+\mu)(1-2\mu)a} \left[\frac{1}{\beta} \frac{\partial \theta_x}{\partial Q} + \frac{\partial \theta_y}{\partial R} \right] \quad (18)$$

$$\tau_{xz} = \frac{E(1-2\mu)ts}{2(1+\mu)(1-2\mu)a} \left[\frac{a}{ts} \theta_x + \frac{1}{ts} \frac{\partial w}{\partial R} \right] \quad (19)$$

$$\tau_{yz} = \frac{E(1-2\mu)ts}{2(1+\mu)(1-2\mu)a} \left[\frac{a}{ts} \theta_y + \frac{1}{\beta ts} \frac{\partial w}{\partial Q} \right] \quad (20)$$

Strain energy. Strain energy is defined as the average of the product of stress and strain indefinitely summed up within the spatial domain of the body. This mathematically expressed as:

$$U = \frac{abt}{2} \int_0^1 \int_0^1 \int_{-0.5}^{0.5} (\sigma_x \varepsilon_x + \sigma_y \varepsilon_y + \sigma_z \varepsilon_z + \tau_{xy} \gamma_{xy} + \tau_{xz} \gamma_{xz} + \tau_{yz} \gamma_{yz}) dR dQ dS \quad (21)$$

Substituting Equations 8 to 13 and Equations 15 to 20 into Equation 21, simplifying and carrying out the integration of the outcome with respect to S gives:

$$U = \frac{D^* ab}{2a^2} \int_0^1 \int_0^1 \left[(1-\mu) \left(\frac{\partial \theta_{sx}}{\partial R} \right)^2 + \frac{1}{\beta} \frac{\partial \theta_{sx}}{\partial R} \cdot \frac{\partial \theta_{sy}}{\partial Q} + \frac{(1-\mu)}{\beta^2} \left(\frac{\partial \theta_{sy}}{\partial Q} \right)^2 + \frac{(1-2\mu)}{2\beta^2} \left(\frac{\partial \theta_{sx}}{\partial Q} \right)^2 + \frac{(1-2\mu)}{2} \left(\frac{\partial \theta_{sy}}{\partial R} \right)^2 \right. \\ \left. + \frac{6(1-2\mu)}{t^2} \left(a^2 \theta_{sx}^2 + a^2 \theta_{sy}^2 + \left(\frac{\partial w}{\partial R} \right)^2 + \frac{1}{\beta^2} \left(\frac{\partial w}{\partial Q} \right)^2 + 2a \theta_{sx} \frac{\partial w}{\partial R} + \frac{2a \theta_{sy}}{\beta} \frac{\partial w}{\partial Q} \right) \right. \\ \left. + \frac{(1-\mu)a^2}{t^4} \left(\frac{\partial w}{\partial S} \right)^2 \right] dR dQ \quad (22)$$

Where:

$$D^* = \frac{Et^3}{12(1+\mu)(1-2\mu)} = D \frac{(1-\mu)}{(1-2\mu)} \quad (23)$$

Total potential energy functional. Total potential energy functional is the algebraic summation of strain energy and external work. That is:

$$\Pi = U - V \quad (24)$$

However, the external work for buckling load is given as:

$$V = \frac{abN_x}{2a^2} \int_0^a \int_0^b \left(\frac{\partial w}{\partial R} \right)^2 dR dQ \quad (25)$$

Substituting Equations 22 and 25 into Equation 24 gives:

$$\Pi = \frac{D^* ab}{2a^2} \int_0^1 \int_0^1 \left[(1-\mu) \left(\frac{\partial \theta_{sx}}{\partial R} \right)^2 + \frac{1}{\beta} \frac{\partial \theta_{sx}}{\partial R} \cdot \frac{\partial \theta_{sy}}{\partial Q} + \frac{(1-\mu)}{\beta^2} \left(\frac{\partial \theta_{sy}}{\partial Q} \right)^2 + \frac{(1-2\mu)}{2\beta^2} \left(\frac{\partial \theta_{sx}}{\partial Q} \right)^2 + \frac{(1-2\mu)}{2} \left(\frac{\partial \theta_{sy}}{\partial R} \right)^2 \right. \\ \left. + \frac{6(1-2\mu)}{t^2} \left(a^2 \theta_{sx}^2 + a^2 \theta_{sy}^2 + \left(\frac{\partial w}{\partial R} \right)^2 + \frac{1}{\beta^2} \left(\frac{\partial w}{\partial Q} \right)^2 + 2a \theta_{sx} \frac{\partial w}{\partial R} + \frac{2a \theta_{sy}}{\beta} \frac{\partial w}{\partial Q} \right) + \frac{(1-\mu)a^2}{t^4} \left(\frac{\partial w}{\partial S} \right)^2 \right. \\ \left. - \frac{N_x}{D^*} \left(\frac{\partial w}{\partial R} \right)^2 \right] dR dQ \quad (26)$$

B. Compatibility Equation

Minimizing the total potential energy functional with respect to rotation in x-z plane and rotation in y-z plane gives the compatibility equations in x-z plane y-z plane respectively:

$$\frac{\partial \Pi}{\partial \theta_{sx}} = \frac{D^* ab}{2a^2} \int_0^1 \int_0^1 \left[(1-\mu) \frac{\partial^2 \theta_{sx}}{\partial R^2} + \frac{1}{2\beta} \frac{\partial^2 \theta_{sy}}{\partial R \partial Q} + \frac{(1-2\mu)}{2\beta^2} \frac{\partial^2 \theta_{sx}}{\partial Q^2} + \frac{6(1-2\mu)}{t^2} \left(a^2 \theta_{sx} + a \frac{\partial w}{\partial R} \right) \right] dR dQ \\ = 0 \quad (27)$$

$$\frac{\partial \Pi}{\partial \theta_{sy}} = \frac{D^* ab}{2a^2} \int_0^1 \int_0^1 \left[\frac{1}{2\beta} \frac{\partial^2 \theta_{sx}}{\partial R \partial Q} + \frac{(1-\mu)}{\beta^2} \frac{\partial^2 \theta_{sy}}{\partial Q^2} + \frac{(1-2\mu)}{2} \frac{\partial^2 \theta_{sy}}{\partial R^2} + \frac{6(1-2\mu)}{t^2} \left(a^2 \theta_{sy} + \frac{a}{\beta} \frac{\partial w}{\partial Q} \right) \right] dR dQ = 0 \quad (28)$$

For Equations 27 and 28 to be true, their integrands must be zero. That is:

$$(1-\mu) \frac{\partial^2 \theta_{sx}}{\partial R^2} + \frac{1}{2\beta} \frac{\partial^2 \theta_{sy}}{\partial R \partial Q} + \frac{(1-2\mu)}{2\beta^2} \frac{\partial^2 \theta_{sx}}{\partial Q^2} + \frac{6(1-2\mu)}{t^2} \left(a^2 \theta_{sx} + a \frac{\partial w}{\partial R} \right) = 0 \quad (29) \quad (31)$$

$$\frac{1}{2\beta} \frac{\partial^2 \theta_{sx}}{\partial R \partial Q} + \frac{(1-\mu)}{\beta^2} \frac{\partial^2 \theta_{sy}}{\partial Q^2} + \frac{(1-2\mu)}{2} \frac{\partial^2 \theta_{sy}}{\partial R^2} + \frac{6(1-2\mu)}{t^2} \left(a^2 \theta_{sy} + \frac{a}{\beta} \frac{\partial w}{\partial Q} \right) = 0 \quad (30) \quad (32)$$

Using law of addition, the Equations 12 and 13 will be simplified and substituted into Equations 29 and 30 respectively, then factorizing the outcome gives:

$$\frac{\partial w}{\partial R} \left[(1-\mu) \frac{\partial^2}{\partial R^2} + \frac{1}{\beta^2} \frac{\partial^2}{\partial Q^2} (1-\mu) + \frac{6(1-2\mu)a^2}{t^2} \cdot \left(1 + \frac{1}{c} \right) \right] = 0 \quad (31)$$

$$\frac{1}{\beta} \frac{\partial w}{\partial Q} \left[\frac{\partial^2}{\partial R^2} (1-\mu) + \frac{(1-\mu)}{\beta^2} \frac{\partial^2}{\partial Q^2} + \frac{6(1-2\mu)a^2}{t^2} \cdot \left(1 + \frac{1}{c} \right) \right] = 0 \quad (32)$$

One of the possibilities of Equation 31 to be true is for the terms in the bracket to sum to zero. Adding terms in the brackets of Equation 31 and 32 gives:

$$\frac{6(1-2\mu)(1+c)}{t^2} = -\frac{c(1-\mu)}{a^2} \left(\frac{\partial^2}{\partial R^2} + \frac{1}{\beta^2} \frac{\partial^2}{\partial Q^2} \right) \quad (33)$$

C. General Governing Equation

The general governing equation is obtained by minimizing the total potential energy functional with respect to deflection. That is:

$$\frac{\partial \Pi}{\partial w} = \frac{D^*}{2a^2} \int_0^1 \int_0^1 \left[\frac{12(1-2\mu)}{t^2} \left(\frac{\partial^2 w}{\partial R^2} + \frac{1}{\beta^2} \frac{\partial^2 w}{\partial Q^2} + a \frac{\partial \theta_{sx}}{\partial R} + \frac{a}{\beta} \frac{\partial \theta_{sy}}{\partial Q} \right) + 2 \frac{(1-\mu)a^2}{t^4} \frac{\partial^2 w}{\partial S^2} - 2 \frac{N_x}{D^*} \frac{\partial^2 w}{\partial R^2} \right] dR dQ = 0 \quad (34)$$

Substituting the simplified Equations 12 and 13 into Equation 34 and simplifying the outcome gives:

$$\frac{D^*}{2a^2} \int_0^1 \int_0^1 \left[\frac{6(1-2\mu)(1+c)}{t^2} \left(\frac{\partial^2 w}{\partial R^2} + \frac{1}{\beta^2} \frac{\partial^2 w}{\partial Q^2} \right) + \frac{(1-\mu)a^2}{t^4} \frac{\partial^2 w}{\partial S^2} - \frac{N_x}{D^*} \frac{\partial^2 w}{\partial R^2} \right] dR dQ = 0 \quad (35)$$

Let:

$$w = w_R \cdot w_Q \cdot w_S \quad (36)$$

$$w = w_1 \cdot w_S \quad (37)$$

$$w_1 = w_R \cdot w_Q \quad (38)$$

$$N_x = N_{x1} + N_{xs} \quad (39)$$

Substituting Equation 37, 38 and 33 into Equation 35 and simplifying the outcome gives:

$$\frac{D^*}{2a^2} \int_0^1 \int_0^1 \left[\left(\frac{\partial^4 w_1}{\partial R^4} + \frac{2}{\beta^2} \frac{\partial^4 w_1}{\partial R^2 \partial Q^2} + \frac{1}{\beta^4} \frac{\partial^4 w_1}{\partial Q^4} - \frac{N_{x1} a^4}{g D^*} \frac{\partial^2 w_1}{\partial R^2} \right) w_S + \frac{w_1}{g} \left(\frac{(1-\mu)a^4}{t^4} \frac{\partial^2 w_S}{\partial S^2} - \frac{N_{xs} a^4}{D^*} \frac{\partial^2 w_S}{\partial R^2} \right) \right] dR dQ = 0 \quad (40)$$

For Equation 40 to be true, its integrand must be zero. That is:

$$\left(\frac{\partial^4 w_1}{\partial R^4} + \frac{2}{\beta^2} \frac{\partial^4 w_1}{\partial R^2 \partial Q^2} + \frac{1}{\beta^4} \frac{\partial^4 w_1}{\partial Q^4} - \frac{N_{x1} a^4}{g D^*} \frac{\partial^2 w_1}{\partial R^2} \right) w_S + \frac{w_1}{g} \left(\frac{(1-\mu)a^4}{t^4} \frac{\partial^2 w_S}{\partial S^2} - \frac{N_{xs} a^4}{D^*} \frac{\partial^2 w_S}{\partial R^2} \right) = 0 \quad (41)$$

One of the possibilities of Eqn. 41 to be true is for the terms in each of the two brackets sum to zero. That is:

$$\frac{\partial^4 w_1}{\partial R^4} + \frac{2}{\beta^2} \frac{\partial^4 w_1}{\partial R^2 \partial Q^2} + \frac{1}{\beta^4} \frac{\partial^4 w_1}{\partial Q^4} - \frac{N_{x1} a^4}{g D^*} \frac{\partial^2 w_1}{\partial R^2} = 0 \quad (42)$$

$$\frac{(1-\mu)a^4}{t^4} \frac{\partial^2 w_S}{\partial S^2} - \frac{N_{xs} a^4}{D^*} \frac{\partial^2 w_S}{\partial R^2} = 0 \quad (43)$$

Eqns. 42 and 43 are the two Governing Equations of a 3-dimensional rectangular plate subject to pure buckling. Thus, the exact solution to the differential equation of Equation 42 is in trigonometric form gives:

$$w_1 = [1 \ R \ \cos(c_1 R) \ \sin(c_1 R)] \begin{bmatrix} a_0 \\ a_1 \\ a_2 \\ a_3 \end{bmatrix} \cdot [1 \ Q \ \cos(c_1 Q) \ \sin(c_1 Q)] \begin{bmatrix} b_0 \\ b_1 \\ b_2 \\ b_3 \end{bmatrix} \quad (44)$$

Recall from Equation 1, $w = A_1 \cdot h$ and w_s is only differential along z-axis. Hence, it is constant along x-axis and y-axis. Thus, Substituting Equation 45 into Equation 37, gives;

$$w = \Delta_0 [1 \ R \ \text{Cos}(c_1 R) \ \text{Sin}(c_1 R)] \begin{bmatrix} a_0 \\ a_1 \\ a_2 \\ a_3 \end{bmatrix} \cdot [1 \ Q \ \text{Cos}(c_1 Q) \ \text{Sin}(c_1 Q)] \begin{bmatrix} b_0 \\ b_1 \\ b_2 \\ b_3 \end{bmatrix} \quad (45)$$

Where:

$$w_s = \Delta_0 + \Delta_1 S \quad (46)$$

And,

$$w_s = \Delta_0 \quad (47)$$

Substituting Equation 45 into the simplified Equations 12 and 13 and simplifying the outcome gives:

$$\theta_{sx} = \frac{c}{a} \cdot \Delta_0 \cdot [1 \ c_1 \text{Sin}(c_1 R) \ c_1 \text{Cos}(c_1 R)] \begin{bmatrix} a_1 \\ a_2 \\ a_3 \end{bmatrix} \cdot [1 \ Q \ \text{Cos}(c_1 Q) \ \text{Sin}(c_1 Q)] \begin{bmatrix} b_0 \\ b_1 \\ b_2 \\ b_3 \end{bmatrix} \quad (48)$$

$$\theta_{sy} = \frac{c}{a\beta} \cdot \Delta_0 \cdot [1 \ R \ \text{Cos}(c_1 R) \ \text{Sin}(c_1 R)] \begin{bmatrix} a_0 \\ a_1 \\ a_2 \\ a_3 \end{bmatrix} \cdot [1 \ c_1 \text{Sin}(c_1 Q) \ c_1 \text{Cos}(c_1 Q)] \begin{bmatrix} b_0 \\ b_1 \\ b_2 \\ b_3 \end{bmatrix} \quad (49)$$

In symbolic forms, Equations 48 and 49 are:

$$\theta_{sx} = \frac{A_{2R}}{a} \cdot \frac{\partial h}{\partial R} \quad (50)$$

$$\theta_{sy} = \frac{A_{2Q}}{a\beta} \cdot \frac{\partial h}{\partial Q} \quad (51)$$

D. Direct Governing Equation

The governing equation is obtained by minimizing the total potential energy functional with respect to deflection coefficient.

Substituting Equations (1), (50) and (51) into Equation (26) gives:

$$\begin{aligned} \Pi = \frac{D^* ab}{2a^4} & \left[(1 - \mu) A_{2R}^2 k_{RR} + \frac{1}{\beta^2} \left[A_{2R} \cdot A_{2Q} + \frac{(1 - 2\mu) A_{2R}^2}{2} + \frac{(1 - 2\mu) A_{2Q}^2}{2} \right] k_{RQ} + \frac{(1 - \mu) A_{2Q}^2}{\beta^4} k_{QQ} \right. \\ & + 6(1 - 2\mu) \left(\frac{a}{t} \right)^2 \left([A_{2R}^2 + A_1^2 + 2A_1 A_{2R}] \cdot k_R + \frac{1}{\beta^2} \cdot [A_{2Q}^2 + A_1^2 + 2A_1 A_{2Q}] \cdot k_Q \right) \\ & \left. - \frac{N_x a^2 A_1^2}{D^*} \cdot k_R \right] \quad (52) \end{aligned}$$

Where:

$$k_{RR} = \int_0^1 \int_0^1 \left(\frac{\partial^2 h}{\partial R^2} \right)^2 dRdQ; \quad k_{RQ} = \int_0^1 \int_0^1 \left(\frac{\partial^2 h}{\partial R \partial Q} \right)^2 dRdQ; \quad k_{QQ} = \int_0^1 \int_0^1 \left(\frac{\partial^2 h}{\partial Q^2} \right)^2 dRdQ;$$

$$k_R = \int_0^1 \int_0^1 \left(\frac{\partial h}{\partial R} \right)^2 dRdQ; \quad k_Q = \int_0^1 \int_0^1 \left(\frac{\partial h}{\partial Q} \right)^2 dRdQ$$

Minimizing Equation 52 with respect to A_{2R} and A_{2Q} and Solving Equations simultaneously gives respectively:

$$A_{2R} = M_2 A_1 \quad (53)$$

$$A_{2Q} = M_3 A_1 \quad (54)$$

Where:

$$M_2 = \frac{(m_{12} m_{23} - m_{13} m_{22})}{(m_{12} m_{12} - m_{11} c_{22})}; \quad M_3 = \frac{(m_{12} m_{13} - m_{11} m_{23})}{(m_{12} m_{12} - m_{11} m_{22})}$$

$$m_{11} = (1 - \mu) k_{RR} + \frac{1}{2\beta^2} (1 - 2\mu) k_{RQ} + 6(1 - 2\mu) \left(\frac{a}{t} \right)^2 k_R$$

$$m_{22} = \frac{(1 - \mu)}{\beta^4} k_{QQ} + \frac{1}{2\beta^2} (1 - 2\mu) k_{RQ} + \frac{6}{\beta^2} (1 - 2\mu) \left(\frac{a}{t} \right)^2 k_Q$$

$$m_{12} = m_{21} = \frac{1}{2\beta^2} k_{RQ}; \quad m_{13} = -6(1 - 2\mu) \left(\frac{a}{t} \right)^2 k_R; \quad m_{23} = m_{32} = -\frac{6}{\beta^2} (1 - 2\mu) \left(\frac{a}{t} \right)^2 k_Q$$

Minimizing Equation 52 with respect to A_1 gives:

$$\frac{\partial \Pi}{\partial A_1} = 6(1 - 2\mu) \left(\frac{a}{t} \right)^2 \left([A_1 + M_2 A_1] \cdot k_R + \frac{1}{\beta^2} \cdot [A_1 + M_3 A_1] \cdot k_Q \right) - \frac{N_x a^2 A_1}{D^*} \cdot k_R = 0 \quad (55)$$

Substituting Equations 53 and 54 into Equation 55 and rearranging gives:

$$\frac{N_x a^2}{D^*} = 6(1 - 2\mu) \left(\frac{a}{t}\right)^2 \left([1 + M_2] + \frac{1}{2} \cdot [1 + M_3] \cdot \frac{k_Q}{k_R} \right) \quad (56)$$

This gives:

$$\frac{a^2 N_x}{E t^3} = \frac{(1 + \mu)}{2} \left(\frac{a}{t}\right)^2 \left([1 + M_2] + \frac{1}{2} \cdot [1 + M_3] \cdot \frac{k_Q}{k_R} \right) \quad (57)$$

III. NUMERICAL ANALYSIS

Considering Fig. 3, the numerical analysis of CSSS rectangular plate will be performed to determine the value of the critical buckling load at various span-thickness ratios. A trigonometric displacement function for the analysis CSSS plate was derived according to author in [17] as presented in Equation (45).

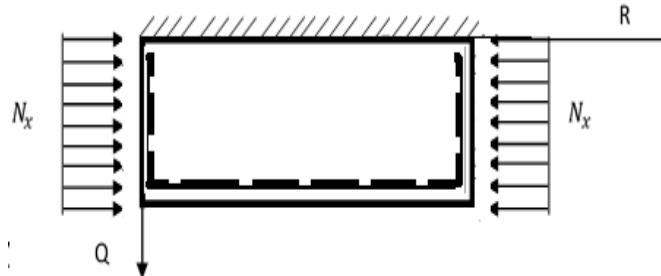


Fig. 3. CSSS Rectangular Plate subjected to uniaxial compressive load.

Equation 45 can be re-written as:

$$w_{(\xi, \epsilon)} = (a_0 + a_1 R + a_2 \cos(c_1 R) + a_3 \sin(c_1 R)) \cdot (b_0 + b_1 Q + b_2 \cos(c_1 Q) + b_3 \sin(Q)) \quad (58)$$

$$\text{At } R = Q = 0; w = 0 \quad (59)$$

$$\text{At } R = Q = 1; M_x \text{ and } M_y \left(\text{ie. } \frac{d^2 w}{dR^2} = \frac{d^2 w}{dQ^2} = 0 \right) \quad (60)$$

$$\text{At } R = Q = 1; U = 0 \quad (61)$$

$$\text{At } Q = 0; Q_x \text{ and } Q_y \left(\text{ie. } \frac{dw}{dQ} = 0 \right) \quad (62)$$

Substituting Equations (59 to 62) into Equation (45) and solving gives the following constants:

$$\sin f_1 = 0; 2 \cos f_1 + f_1 \sin f_1 - 2 \quad (63)$$

The value of f_1 that satisfies Equation (61) is:

$$f_1 = m\pi \text{ [where } m = 1, 2, 3 \dots]; f_1 = 4.49340946 \quad (64)$$

Substituting Equation (64) into (45) and its differentials thereby satisfying the boundary conditions of equation (59 to 63) gave;

$$a_0 = a_1 = a_2 = 0; b_0 = f_1 b_3; b_0 = -f_1 b_3 \quad (65)$$

Substituting the constants of Equation (67) into Equation (47) gives;

$$w = a_3 \sin(\pi R) \times b_3 (f_1 - f_1 Q - f_1 \cos f_1 Q + \sin f_1 Q) \quad (66)$$

That is:

$$U = a_3 \times b_3 (\sin \pi R) \cdot (f_1 - f_1 Q - f_1 \cos f_1 Q + \sin f_1 Q) \quad (67)$$

Recall from Equation 26, that;

$$w = h \cdot A_1$$

Let the amplitude,

$$A_1 = a_3 \times b_3 \quad (68)$$

And;

$$h = (\sin \pi R) \cdot (f_1 - f_1 Q - f_1 \cos f_1 Q + \sin f_1 Q) \quad (69)$$

Thus, the trigonometric deflection functions after satisfying the boundary conditions is

$$w = (\sin \pi R) \cdot (f_1 - f_1 Q - f_1 \cos f_1 Q + \sin f_1 Q) \cdot A_1 \quad (70)$$

IV. RESULTS AND DISCUSSIONS

The result of stiffness coefficients for deflection of rectangular thick analysis subjected to of CSSS boundary condition were obtained using the trigonometric functions as obtained in Equation 70 and presented in Table 1. The Poisson's ratio of the plate is 0.25.

Table 1: The trigonometric stiffness coefficients of deflection function for CSSS plate.

Deflection form	k_{RR}	k_{RQ}	k_{QQ}	k_R	k_Q	k_q
Trigonometry	CSSS	928.2428	1,015.280	2,057.980	94.05066	102.8692

The expression of the critical buckling load $\left(\frac{N_x a^2}{\pi^2 D} \text{ and } \frac{a^2 N_x}{E t^3} \right)$ was obtained in the previous section and the numerical values, determined using Equation 58 and 59 respectively. Table 2 and 3 contains the result of the non-dimensional **Onyeka et al., International Journal on Emerging Technologies 12(1): 228-240(2021) 234**

values of the critical buckling load for an isotropic rectangular thick plate elastically restrained along one the edges and other three edges simply supported (CSSS) under uniaxial compressive load at varying aspect ratio. For the non-dimensional values obtained in Table 3 and 4, it reveals that the values of critical buckling load increase as the span- thickness ratio increases. This load increase continues until failure occurs. This means that a decrease in plate thickness increases the chance of failure in a plate structure. This means that the plate structure is not safe and needed to be maintained. To avoid this, the designer should consider higher thickness or increase the span-thickness ratio of the plate. Furthermore, it can be deduced that as the in-plane load on the plate increase and approaches the critical buckling, the failure in a plate structure is a bound to occur.

Table 2: Non-dimensional Critical Buckling Load $\frac{N_x a^2}{\pi^2 D}$ on the CSSS Rectangular Plate Using Trigonometric Function.

$\frac{a}{t}$	$N_{xcr} = \frac{N_x a^2}{\pi^2 D}$								
	$\beta = 1.0$	$\beta = 1.5$	$\beta = 2.0$	$\beta = 2.5$	$\beta = 3.0$	$\beta = 3.5$	$\beta = 4.0$	$\beta = 4.5$	$\beta = 5.0$
4	4.3145	2.1634	1.5734	1.3356	1.2166	1.1484	1.1057	1.0771	1.0570
5	4.8168	2.3330	1.6761	1.4151	1.2854	1.2115	1.1652	1.1343	1.1126
10	5.7053	2.6057	1.8359	1.5371	1.3903	1.3072	1.2553	1.2208	1.1966
15	5.9076	2.6634	1.8689	1.5621	1.4117	1.3266	1.2736	1.2383	1.2135
20	5.9818	2.6842	1.8807	1.5710	1.4193	1.3335	1.2801	1.2445	1.2196
30	6.0361	2.6993	1.8892	1.5774	1.4248	1.3385	1.2848	1.2490	1.2239
40	6.0553	2.7046	1.8922	1.5797	1.4267	1.3403	1.2864	1.2506	1.2255
50	6.0642	2.7071	1.8936	1.5807	1.4276	1.3411	1.2872	1.2513	1.2262
60	6.0691	2.7084	1.8944	1.5813	1.4281	1.3415	1.2876	1.2517	1.2266
70	6.0720	2.7092	1.8949	1.5817	1.4284	1.3418	1.2879	1.2519	1.2268
80	6.0739	2.7097	1.8952	1.5819	1.4286	1.3419	1.2880	1.2521	1.2269
90	6.0752	2.7101	1.8954	1.5820	1.4287	1.3421	1.2881	1.2522	1.2270
100	6.0762	2.7103	1.8955	1.5821	1.4288	1.3422	1.2882	1.2523	1.2271
1000	6.0801	2.7114	1.8961	1.5826	1.4292	1.3425	1.2886	1.2526	1.2274
1500	6.0802	2.7114	1.8961	1.5826	1.4292	1.3425	1.2886	1.2526	1.2274

Table 3: Non-dimensional Critical Buckling Load $\frac{N_x a^2}{Et^3}$ on the CSSS Rectangular Plate using Trigonometric Function.

$\frac{a}{t}$	$N_{xcr} = \frac{N_x a^2}{Et^3}$								
	$\beta = 1.0$	$\beta = 1.5$	$\beta = 2.0$	$\beta = 2.5$	$\beta = 3.0$	$\beta = 3.5$	$\beta = 4.0$	$\beta = 4.5$	$\beta = 5.0$
4	3.7851	1.8979	1.3804	1.1717	1.0673	1.0075	0.9700	0.9450	0.9273
5	4.2258	2.0467	1.4704	1.2414	1.1277	1.0628	1.0223	0.9952	0.9761
10	5.0052	2.2860	1.6106	1.3485	1.2197	1.1468	1.1013	1.0710	1.0497
15	5.1827	2.3366	1.6396	1.3704	1.2385	1.1638	1.1173	1.0863	1.0646
20	5.2479	2.3549	1.6499	1.3782	1.2452	1.1699	1.1230	1.0918	1.0699
30	5.2954	2.3681	1.6574	1.3839	1.2500	1.1743	1.1271	1.0957	1.0737
40	5.3123	2.3727	1.6601	1.3859	1.2517	1.1758	1.1286	1.0971	1.0751
50	5.3201	2.3749	1.6613	1.3868	1.2525	1.1765	1.1293	1.0978	1.0757
60	5.3244	2.3761	1.6620	1.3873	1.2529	1.1769	1.1296	1.0981	1.0761
70	5.3270	2.3768	1.6624	1.3876	1.2531	1.1771	1.1298	1.0983	1.0763
80	5.3286	2.3772	1.6626	1.3878	1.2533	1.1773	1.1300	1.0985	1.0764
90	5.3298	2.3776	1.6628	1.3879	1.2534	1.1774	1.1301	1.0986	1.0765
100	5.3306	2.3778	1.6629	1.3880	1.2535	1.1775	1.1301	1.0986	1.0765
1000	5.3341	2.3787	1.6635	1.3884	1.2539	1.1778	1.1304	1.0989	1.0768
1500	5.3341	2.3787	1.6635	1.3884	1.2539	1.1778	1.1304	1.0989	1.0768

Looking closely at Fig. 4 to 12, which shows that the results of the critical buckling load of an isotropic rectangular thick plate elastically restrained along one the edge and other three edges simply supported (CSSS) under uniaxial compressive load at varying aspect ratio. It reveals that the increase in the value of the length-breadth ratio ($\beta = 1.0, 1.5, 2.0, 2.5, 3.0, 3.5, 4.0, 4.5$ and 5.0) decreases the value of the critical buckling load N_x . This continued until safety is ensured in the plate structure. In the result, it is observed that an increase in plate width increases the chance of failure in a plate structure. To maintain this, the designer should consider higher plate width or decrease the length-breadth ratio of the plate.

In summary, Table 4 to 5 and figure 4 to 10 presented here, it is observed that as the in-plane load which will cause the plate to fail by compression increases from zero to critical buckling load (N_{xcr}), the buckling of the plate exceed specified elastic limit thereby causing failure in the plate structure. This means that, the load that causes the plate to deform also causes the plate material to buckle simultaneously.

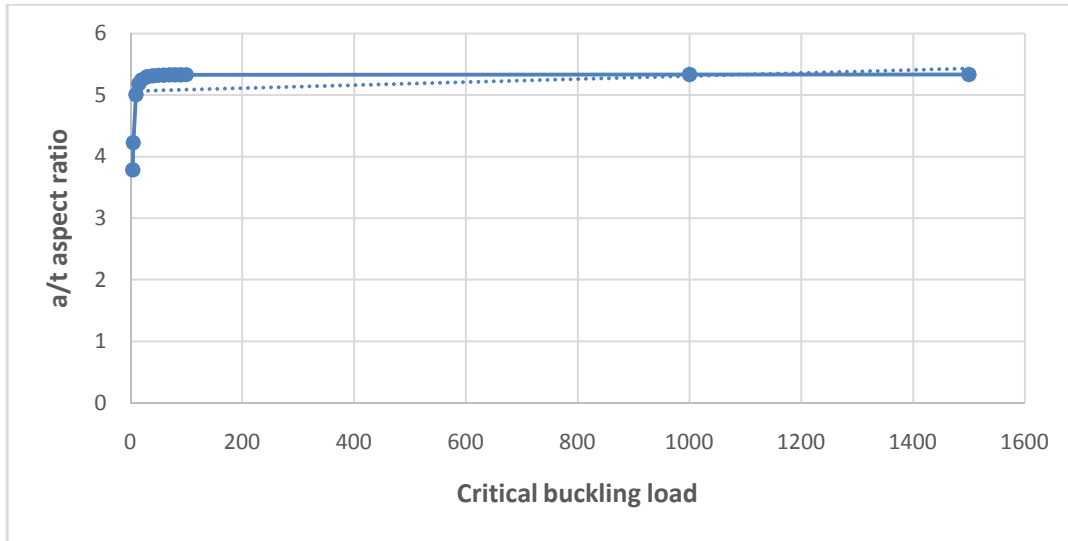


Fig. 4. Graph of Critical buckling load versus aspect ratio of a square rectangular plate.

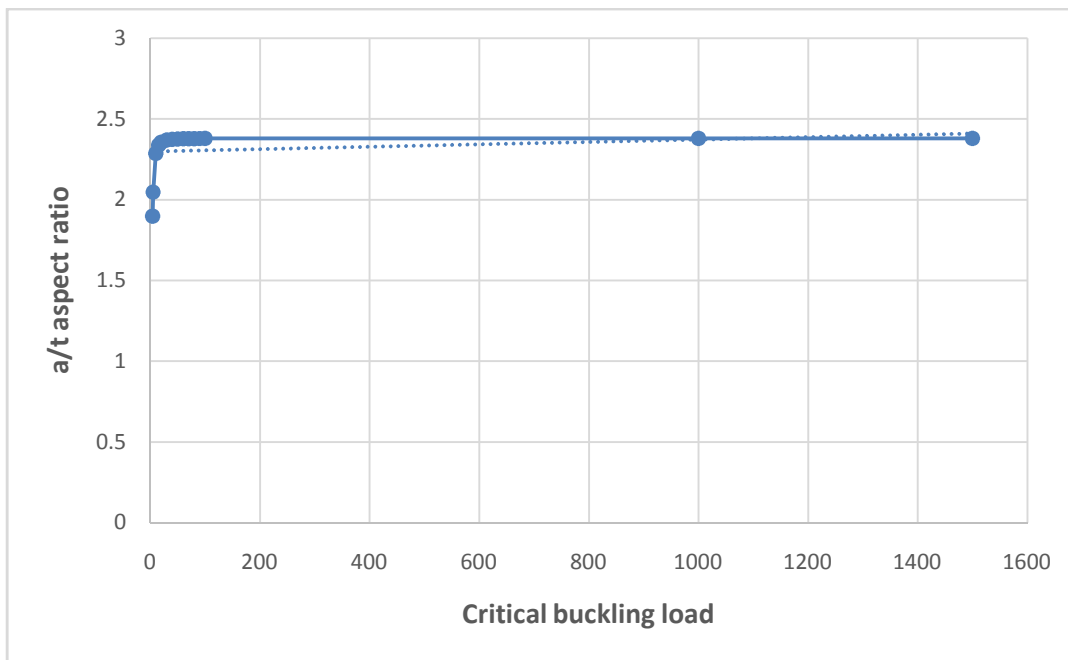


Fig. 5. Graph of Critical buckling load versus aspect ratio of plate at length-to-breadth ratio of 1.5.

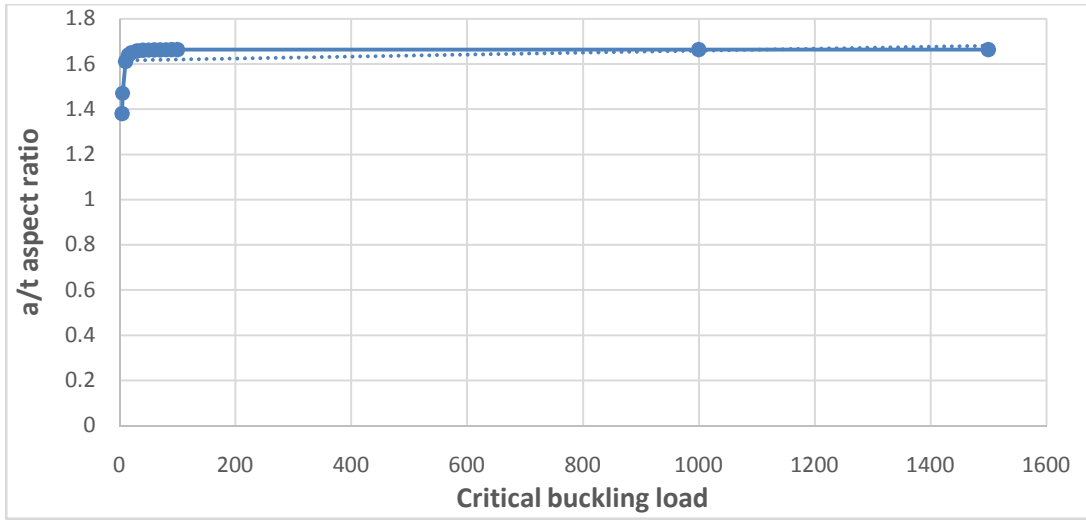


Fig. 6. Graph of Critical buckling load versus aspect ratio of plate at length-to-breadth ratio of 2.0.

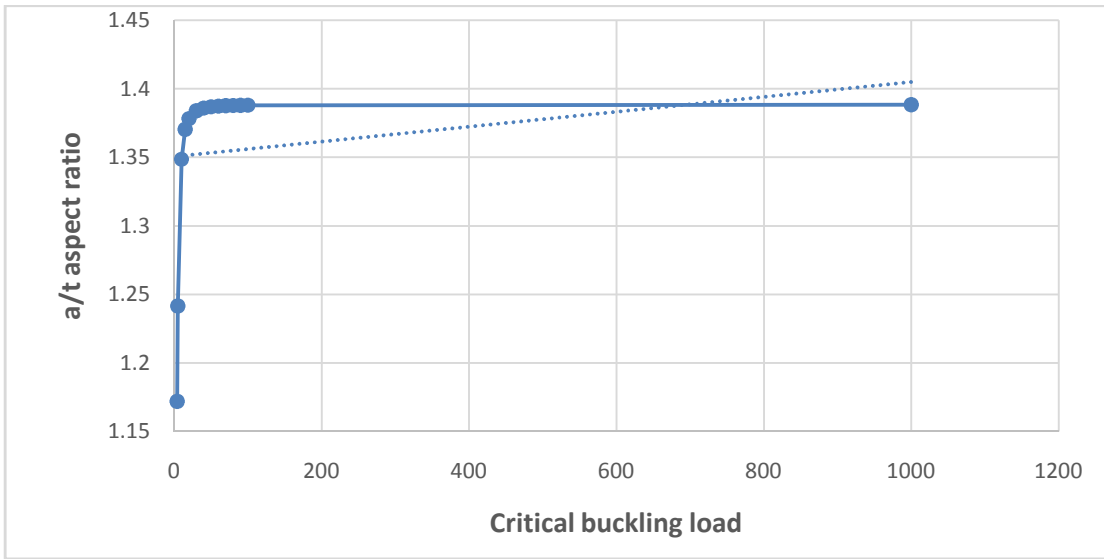


Fig. 7. Graph of Critical buckling load versus aspect ratio of plate at length-to-breadth ratio of 2.5.

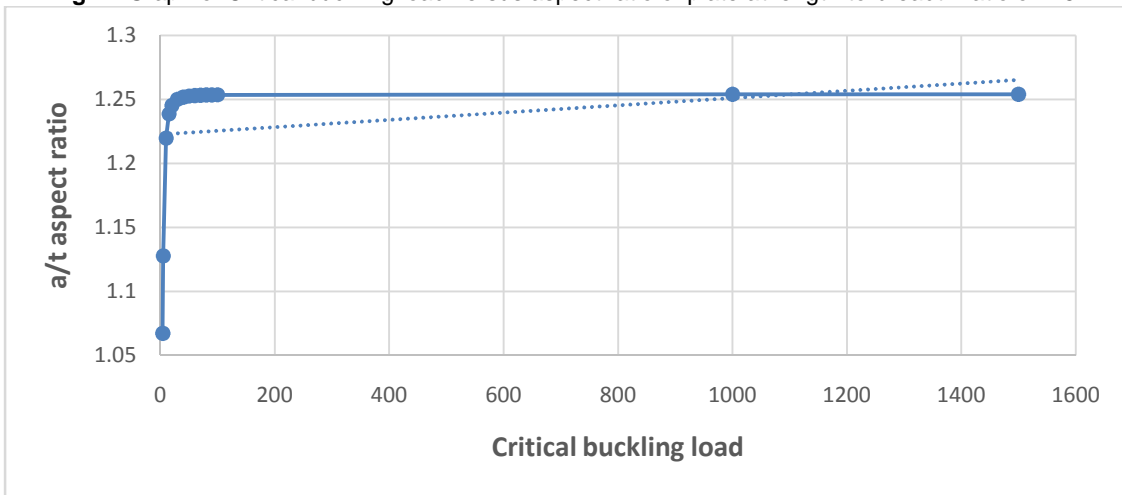


Fig. 8. Graph of Critical buckling load versus aspect ratio of plate at length-to-breadth ratio of 3.0

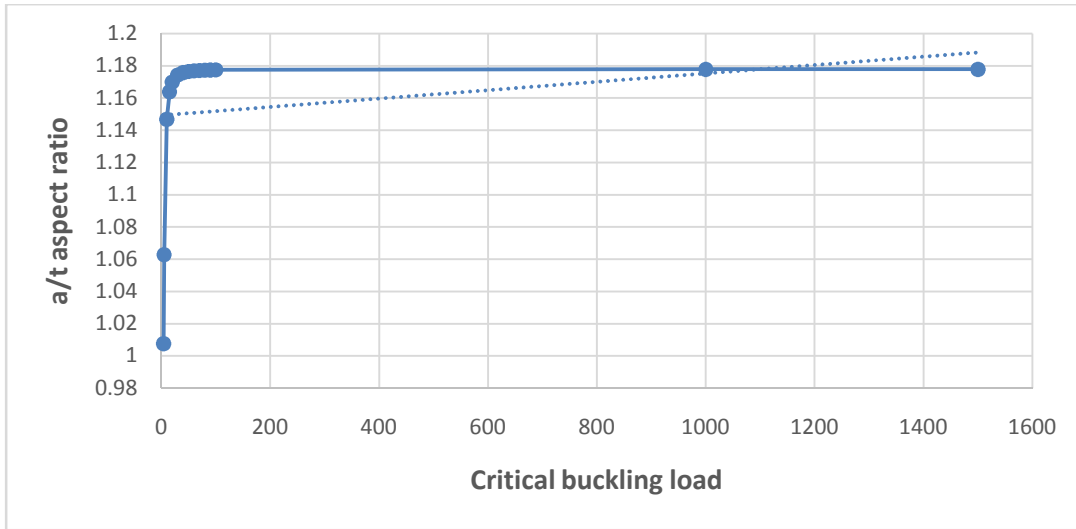


Fig. 9. Graph of Critical buckling load versus aspect ratio of plate at length-to-breadth ratio of 3.5

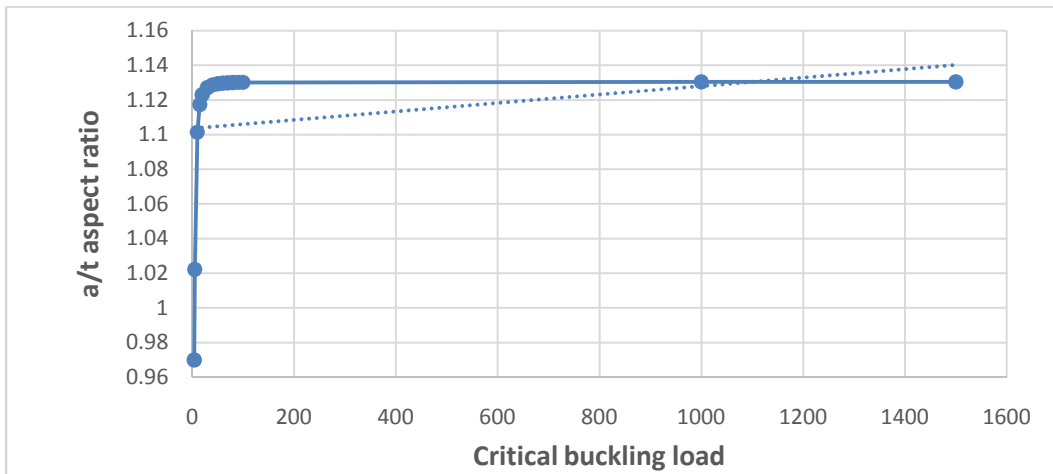


Fig. 10. Graph of Critical buckling load versus aspect ratio of plate at length-to-breadth ratio of 4.0.

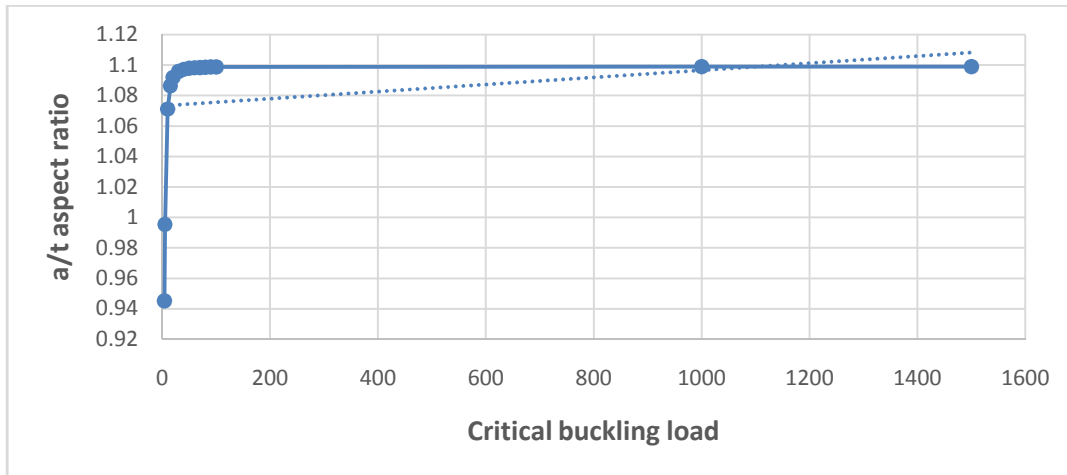


Fig. 11. Graph of Critical buckling load versus aspect ratio of plate at length-to-breadth ratio of 4.5

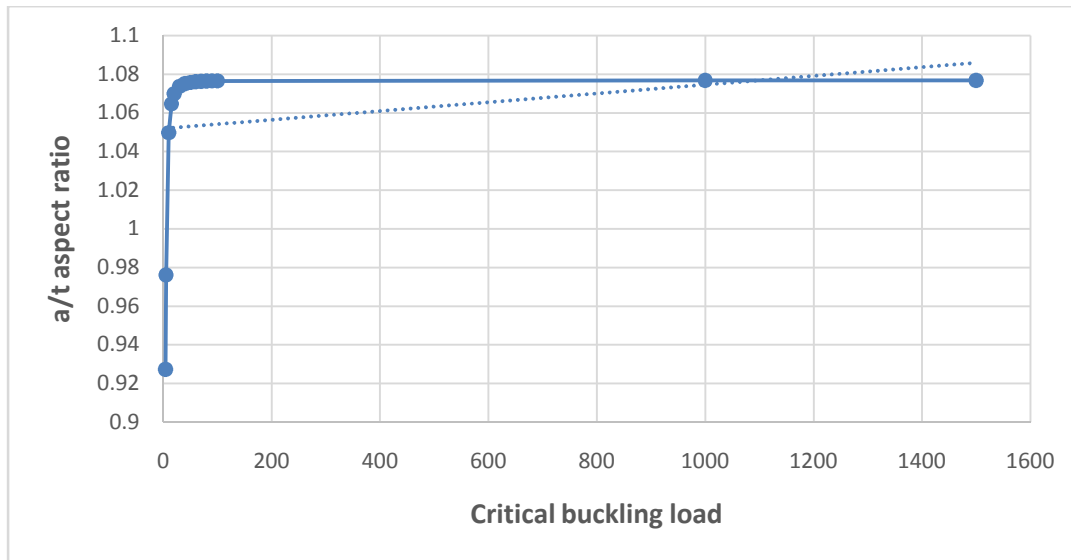


Fig. 12. Graph of Critical buckling load versus aspect ratio of plate at length-to-breadth ratio of 5.0

V. CONCLUSION AD RECOMMENDATION

It can be concluded that the classical theory is good for thin plates but over-predicts buckling loads in relatively thick plates. Hence, the incomplete three-dimensional shear deformation theory is only an approximate relation for buckling analysis of thick plate (although it turns out to be exact in the case of pure bending). Furthermore, the trigonometric displacement functions developed were derived from the compatibility equation obtained from first principle and their use in the analysis of thick plates will yield exact results. Thus, the displacement functions developed in this work are recommended for use in analysis of isotropic thick rectangular plates.

Data Availability Statement: All data, models, or code that support the findings of this study are available from the corresponding author upon reasonable request.

REFERENCES

- [1]. Chandrashekhara, K., (2001). Theory of Plates. *University Press (India) Limited*.
- [2]. Timoshenko, S. and Gere, J. M., (1963). Theory of Elastic Stability, 2nd Edition. *McGraw-Hill Books Company*, New York,
- [3]. Kirchhoff, G.R., (1850). U"ber das Gleichgewicht and die Bewe gung einerelastschen Scheibe. *Journal f" ur die reine und angewandteMathematik*, Vol. 40: 51-88 (in German).
- [4]. Tehrani, B.T, and Kabir, M.Z., (2016). Buckling of Rectangular Plates Partially Restrained along Opposite Edges. *3rd National & 1st International Conference on Applied Research in Electrical, Mechanical & Mechatronics Engineering*.
- [5]. Zenkour A.M., (2003). Exact Mixed-Classical Solutions for the Bending Analysis of Shear Deformable Rectangular Plates. *Applied Mathematical Modelling*, Vol. 27(7): 515-534.
- [6]. Ibearugbulem, O.M., (2016). Note on Rectangular Plate Analysis. *Lambert Academic Publishing*.
- [7]. Reissner, E., (1945). The Effect of Transverse Shear Deformations on the Bending of Elastic Plates. *ASME Journal of Applied Mechanics*, Vol. 12: A69-A77.
- [8]. Mindlin. R.D., (1951). Influence of Rotary Inertia and Shear on Flexural Motion of Isotropic Elastic Plates. *ASME Journal of Applied Mechanics*, Vol. 18: 31-38.
- [9]. Shufrin and Eisenberger, M., (2005). Stability and Vibration of Shear Deformable Plates - First order and Higher Order Analyses. *International Journal of Solids and Structures*, Vol. 42(3-4): 1225–1251.
- [10]. Sayyad, A.S. and Ghugal, Y.M., (2012). Buckling Analysis of Thick Isotropic Plates by Using Exponential Shear Deformation Theory. *Applied and Computational Mechanics*, Vol. 6:185-196.
- [11]. Ghugal, Y.M. and Pawar, M.D., (2011). Buckling and Vibration of Plates by Hyperbolic Shear Deformation Theory. *Journal of Aerospace Engineering and Technology*, Vol. 1(1): 1–12.
- [12]. Gunjal, S.M., Hajare, R.B., Sayyad, A.S. and Ghodle, M.D., (2015). Buckling Analysis of Thick Plates using Refined Trigonometric Shear Deformation Theory. *Journal of Materials and Engineering Structures*, Vol. 2: 159–167.
- [13]. Ezeh, J.C., Onyechere, I.C., Ibearugbulem, O.M., Anya, U.C. and Anyaogu, L., (2018). Buckling Analysis of Thick Rectangular Flat SSSS Plates using Polynomial Displacement Functions. *International Journal of Scientific & Engineering Research*, Vol. 9(9): 387- 392.
- [14]. Onyeka, F.C., Okafor, F.O., Onah, H.N., (2018). Displacement and Stress Analysis in Shear Deformable Thick Plate. *International Journal of Applied Engineering Research* Vol. 13(11): 9893-9908.

- [15]. Onyeka, F.C., Okafor, F.O., Onah, H.N., (2019). Application of Exact Solution Approach in the Analysis of Thick Rectangular Plate. *International Journal of Applied Engineering Research* Vol. 14(8): 2043-2057.
- [16]. Vareki, A.M., Neya, B.N. and Amiri, J.V., (2016). 3-D Elasticity Buckling Solution for Simply Supported Thick Rectangular Plates using Displacement Potential Functions. *Applied Mathematical Modelling*, Vol. 40: 5717–5730.
- [17]. Onyeka, F.C., Osegbowa, D. and Arinze, E.E., (2020). Application of a New Refined Shear Deformation Theory for the Analysis of Thick Rectangular Plates. *Nigerian Research Journal of Engineering and Environmental Sciences*, Vol. 5(2): 901-917.

How to cite this article: Onyeka, F.C., Okafor, F.O. and Onah H.N. (2021). Application of a New Trigonometric Theory in the Buckling Analysis of Three-Dimensional Thick Plate. *International Journal of Emerging Technologies*, 12(1): 228–240.